Copyright 2001 by the Society of Photo-Optical Instrumentation Engineers.

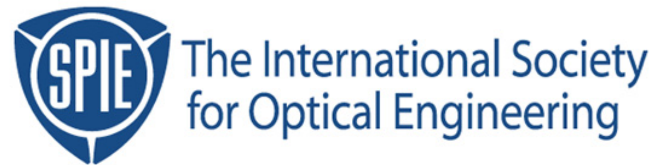

This paper was published in the proceedings of
Lithography for Semiconductor Manufacturing
SPIE Vol. 4404, pp. 111-122.
It is made available as an electronic reprint with permission of SPIE.

One print or electronic copy may be made for personal use only. Systematic or multiple reproduction, distribution to multiple locations via electronic or other means, duplication of any material in this paper for a fee or for commercial purposes, or modification of the content of the paper are prohibited.

Towards a Universal Resist Dissolution Model for Lithography Simulation

Stewart Robertson
Shipley Company Inc., 455 Forest Street, Marlborough, MA 01752

Chris Mack and Mark Maslow
Parametric Solutions Division, KLA-Tencor Corporation,
8834 North Capital of Texas Highway, Suite 301, Austin, TX 78859

ABSTRACT

In lithography simulation dissolution rate equations are used to map development rate to the resist latent image. This work examines the quality of fit of four rate equations to experimental dissolution data for a wide variety of different resists ranging from medium contrast i-line novolak/DNQ materials to the state-of-the-art 248nm and 193nm chemically amplified photoresists. Three of the rate equations are routinely used for modeling; the Mack rate equation, the Enhanced Mack rate equation, and the Notch rate equation. The fourth is the recently developed Enhanced Notch model. Although each class of photoresist can be fitted reasonably well by one of the conventional rate equations, the Enhanced Notch model yields the best fit to the experimental data in all cases.

Keywords: *lithography simulation, dissolution model, rate equation*

1. INTRODUCTION

All current lithography modeling is based on the pioneering work of Dill *et al*.[1-4] Although more complex model details have been introduced to describe modern processing practices, commercial simulation packages still utilize the techniques and principles laid down by Dill and his coworkers in 1975.

They proposed that a lithographic process could be modeled in two separate stages, exposure and development. During exposure, knowledge of the exposure tool's optical configuration and the mask pattern is used to construct an aerial image. This image is used in conjunction with optical information about the substrate and the resist to calculate the distribution of DNQ PAC (photoactive compound or inhibitor) within the novolak film. This distribution is usually referred to as the latent image. During development, the rate of resist dissolution is considered to be solely related to the instantaneous inhibitor concentration at the developer interface; thus, an iterative approach with respect to develop time allows a resist profile to be evolved from the latent image.

Since Dill's original work, lithographic processes have changed, necessitating some additional modeling steps. The first major process innovation was the introduction of the post exposure bake (PEB) to remove standing wave artifacts from resist profiles. The primary lithographic impact of the PEB is thermally driven inhibitor diffusion, which can be modeled by applying Fick's second law of diffusion to the latent image[5]. The second major process change was the advent of chemically amplified, or acid catalyzed, photoresists when 248 nm exposure tools were introduced. As the chemistry of these materials is significantly different from that of their novolak/DNQ predecessors, model alterations were required. The exposure step now calculates the distribution of photoacid within the resist film. During the PEB, both acid diffusion and acid catalyzed deprotection are calculated simultaneously in an iterative fashion. The resulting distribution of deprotected polymer forms the latent image, and it is the level of deprotection that must be mapped to dissolution rate.

In order to accurately predict the performance of a given resist process, it is important to determine appropriate modeling parameters for that material. Some of these parameters can be measured in a straightforward manner, such as refractive index and bleachable and non-bleachable absorbance, whilst some are very difficult to measure directly, such as diffusivity or deprotection reaction order (these values are usually inferred from indirect evidence).

This work concentrates on the mapping of dissolution rate to the variable controling dissolution, either relative inhibitor concentration or relative blocking level. Typically, this mapping can be determined with a high degree of accuracy; however, it is usual to then fit one of a number of standard "rate equations" to this data. Whilst the equations fit many experimental datasets well, they occasionally yield a completely inappropriate result and often miss subtle but important aspects of dissolution behavior.

2. MAPPING DISSOLUTION RATE TO RELATIVE INHIBITOR CONCENTRATION

2.1 Dissolution Rate Measurements for Novolak/DNQ Photoresists

Samples of four i-line resists were prepared on a 150nm organic anti-reflectant layer (XHRi from Brewer Science Inc., Rolla, MO) according to the conditions described in Table I. The coatings were spun on 150 mm silicon substrates using a DNS-60A track system. Blanket exposed areas ranging in dose from 0 – 750 mJ/cm^2 were created using a GCA XLS-7500 Stepper. Dissolution rate as a function of resist depth was determined for each area using a Perkin-Elmer 5900 DRM (Development Rate Monitor) and custom analysis software. The relative inhibitor concentration (M) as a function of depth and exposure dose was then calculated using ProDRM v5.1m (KLA-Tencor Inc.) based upon optical parameters previously determined for each resist. The M values and dissolution rates were then paired appropriately, excluding the top and bottom 10% of the film. The use of the anti-reflectant layer helps minimize any error incurred from an inaccurate diffusivity estimate.

Resist	SPR®500	SPR®850	SPR®660	Ultra-i® 123
Film Thickness	1048 nm	1000 nm	1000 nm	1000 nm
Softbake	60 Sec @ 95°C	60 Sec @ 90°C	60 Sec @ 90°C	60 Sec @ 90°C
PEB	60 Sec @115°C	60 Sec @ 110°C	60 Sec @ 110°C	60 Sec @ 110°C
Developer	MF®-501	MF® CD-26	MF® CD-26	MF® CD-26

Table I: Processing conditions for the i-line Novolak/DNQ photoresist samples.

2.2 Dissolution Rate Measurements for Chemically Amplified Photoresists

Samples of three chemically amplified resists were prepared on organic anti-reflectant materials according to the conditions described in Table II. The coatings were spun on 200 mm silicon substrates using a TEL Mk8 track system. Blanket exposed areas ranging in dose from 0 – 100 mJ/cm^2 were created using a GCA XLS-7800 stepper for the 248nm samples and an ISI Microstepper for the 193nm sample. Dissolution rate as a function of resist depth was determined for each area using a Lithotech Japan RDA-790 Development Rate Monitor and custom analysis software. The relative blocking level (M) as a function of depth and exposure dose was then calculated using ProDRM v5.1m (KLA-Tencor Inc.) based upon physical and optical parameters previously determined for each resist. The M values and dissolution rates were then paired appropriately, again excluding the top and bottom 10% of the film.

Resist	UV®113	UV®26	EPIC V5
Exposure λ	248 nm	248 nm	193 nm
Film Thickness	798 nm	925 nm	447 nm
ARC	60 nm AR3™	60 nm AR3™	82 nm AR™ 19
Softbake	60 Sec @ 120°C	60 Sec @ 130°C	90 Sec @ 120°C
PEB	60 Sec @ 130°C	90 Sec @ 110°C	60 Sec @ 120°C
Developer	LDD-26W	MF® CD-26	MF® CD-26

Table II: Processing conditions for the chemically amplified photoresist samples.

2.3 Rate Equations

Rather than directly utilizing the dissolution rate versus M mapping that has been determined from the DRM data, it is more typical to fit a 'standard' rate equation to the data and describe the material's development characteristics with a number of parameters. A rate equation is a direct function of M and represents the dissolution behavior in the bulk of the resist. Many resists exhibit either inhibited or enhanced dissolution behavior near their surface. In such cases, the rate equation, *R(M)*, is multiplied by a surface rate modifier (which is a function of M and z, the depth from the upper resist surface); such that[6]

$$Rate(z, M) = f(z, M).R(M) \tag{1}$$

where *f(z,M)* is the surface rate modifier, typically of form[6]

$$f(z, M) = 1 - (1 - f(0, M))e^{-\frac{z}{L}} \tag{2}$$

where *L* is the characteristic depth of surface rate behavior and *f(0,M)* is a function describing the ratio of the development rate at the surface to that in the bulk, as a function of M. Although various *f(0,M)* functions have been proposed[6,7] it is more common for a constant value, independent of M, to be substituted[8]. This work only considers the bulk behavior of the materials being analyzed and the experimental surface data is excluded.

Many rate equations have been proposed[2, 4-16]; however, most published resist models utilize only three of these: the original Mack rate equation, the Enhanced Mack rate equation, and the Notch rate equation. The most important criterion in choosing a development rate equation is how accurately it describes the material's experimentally determined behavior.

In the following subsections, the three commonly used rate equations and the Enhanced Notch rate equation are described.

2.3.1 The Original Mack Kinetic Development Model Rate Equation

Mack[8] proposed a kinetic resist development model for novolak/DNQ photoresists, which has a rate equation of the form:

$$R(M) = R_{\max}\frac{(a+1)(1-M)^n}{a+(1-M)^n} + R_{\min} \tag{3}$$

$$a = \frac{n+1}{n-1}(1-M_{th})^n \tag{4}$$

where R_{max} is the maximum development rate (where all the inhibitor has been photolyzed), R_{min} is the minimum development rate (where the resist is unexposed), M_{th} is the threshold M concentration, where dissolution "turns on" and n is the developer selectivity.

2.3.2 The Enhanced Mack Kinetic Development Model Rate Equation

Mack[14,15] proposed a second kinetic model development model for novolak/DNQ photoresists, which has a rate equation of the form:

$$R(M) = R_{resin} \frac{1 + k_{enh}(1 - M)^n}{1 + k_{inh}(M)^l} \quad (5)$$

$$R_{min} = \frac{R_{resin}}{1 + k_{inh}}$$

(6)

$$R_{max} = R_{resin}(1 + k_{enh}) \quad (7)$$

where R_{min} and R_{max}, are respectively the minimum and maximum development rates, R_{resin} is the development rate of the resin alone, n is enhancement reaction order and l is the inhibition reaction order.

2.3.3 Notch Development Model Rate Equation

Mack and Arthur[10,11] proposed a modification to the original Mack model where a "notch" is added, to describe the type of behavior exhibited by high resolution novolak/DNQ phtoresists. The resulting rate equation has a form of:

$$R(M) = R_{max}(1 - M)^n \left[\frac{(a+1)(1-M)^{n_notch}}{a + (1-M)^{n_notch}} \right] + R_{min} \quad (8)$$

$$a = \frac{(n_notch + 1)}{(n_notch - 1)}(1 - M_{th_notch})^{n_notch} \quad (9)$$

where R_{max}, R_{min}, are again the maximum and minimum development rates, respectively, n is the developer selectivity, M_{th_notch} represents the relative inhibitor concentration where the "notch" occurs and n_notch is the selectivity of the "notch".

2.3.4 Enhanced Notch Model Rate Equation

Robertson *et al.*[16] proposed an enhancement to the Notch model to improve the fit for high resolution novolak/ DNQ photoresists. The resulting Enhanced Notch rate equation is

$$R(M) = R_{max}(1 - M)^n \left[\frac{(a+1)(1-M)^{n_notch}}{a + (1-M)^{n_notch}} \right] + R_{min} \left[\frac{S}{S^M} \right] \cdot \left[1 - \frac{(a+1)(1-M)^{n_notch}}{a + (1-M)^{n_notch}} \right]^2 \quad (10)$$

$$a = \frac{(n_notch + 1)}{(n_notch - 1)}(1 - M_{th_notch})^{n_notch} \quad (11)$$

The parameters have the same meaning as in the standard Notch equation and the new parameter S is defined by :

$$S = \frac{R'_{max}}{R_{min}} \quad (12)$$

where R'_{max} is the development rate at M = 0, of the linear extrapolation of the low dissolution rates above M_{th_notch} on the dissolution rate versus M mapping when dissolution rate is plotted on a logarithmic scale, as illustrated in Figure 1.

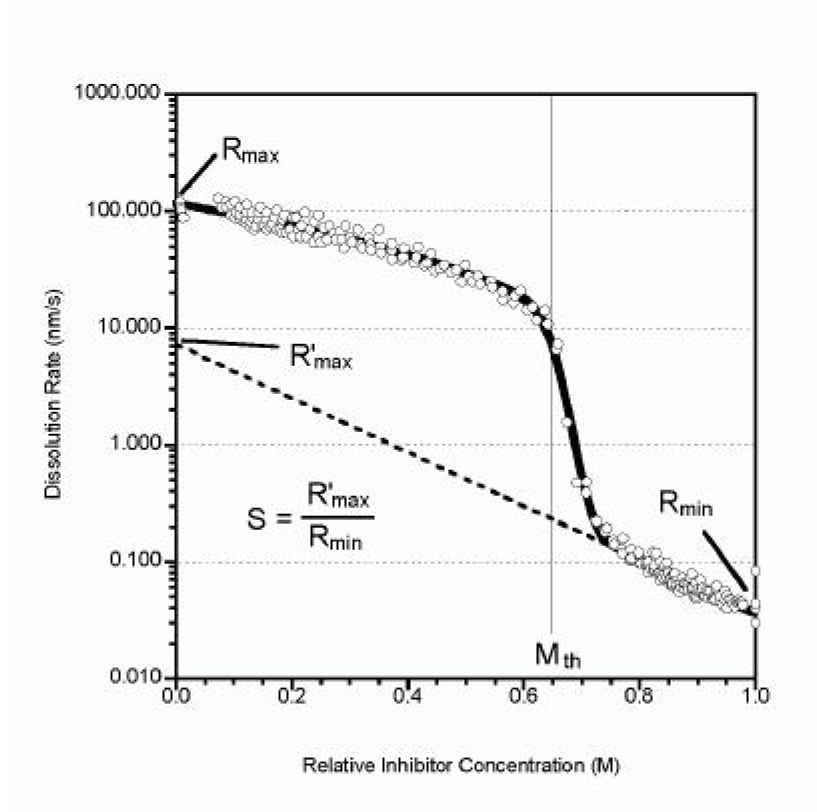

Figure 1: Definition of S and R'_{max} for the Enhanced Notch equation.

2.4 Fitting Rate Equation to Experimental Data

In this work, optimum values for the rate equation parameters are determined using the solver plug-in for Excel (Microsoft Corporation). The rate equation parameters are varied iteratively until the total mean squared error between the equation and the experimental data is minimized. Since a resist's performance is most sensitive to variations in low dissolution rates, a logarithmic weighting is applied to prevent the high rates from dominating the fit.

Once optimum fits have been determined for each rate equation, the root mean squared error (RMSE) between that fit and the experimental data is calculated. The RMSE indicates which of the rate equations best describes the process under analysis.

3. RESULTS OF RATE EQUATION FITTING

3.1 Medium Resolution i-line Novolak/DNQ Photoresists

The SPR®500 and SPR®850 series photoresists are medium resolution i-line materials designed for critical dimensions of 500nm and 400nm, respectively. Table III details the parameter values which give optimum fits for each of the four rate equations for the SPR®500 data. Table IV shows the same information for the SPR®850 data.

In both cases the Enhanced Mack model is the best of the three standard rate equations. This is unsurprising since this class of resist predominated state-of-the-art lithography at the time the model was proposed. The original Mack and Notch models give adequate but not excellent fits to the experimental data. For both materials, it is the Enhanced Notch rate equation that duplicates the observed behavior most accurately.

It is worth noting that all the models do an adequate job of describing these materials and the Enhanced Notch model is only marginally superior to the Enhanced Mack Model. Figure 2 compares the SPR®500/MF®-501 experimental results with the

two best fitting rate equations, (a) the Enhanced Mack and (b) the Enhanced Notch models, respectively. Likewise Figure 3 shows the SPR®850/MF® CD-26 data with the two best fitting rate equations.

3.2 High Resolution i-line Novolak/DNQ Photoresists

The SPR®660 and Ultra-i® 123 series photoresists are high resolution i-line materials designed for critical dimensions of 300nm and 250nm, respectively. Table V details the parameter values which give optimum fits for each of the four rate equations for the SPR®660 data. Table VI shows the same information for the Ultra-i® 123 data.

Both of these materials exhibit the "notch" behavior first described by Arthur[9,10], typical of such high resolution materials. For the Ultra-i® 123 the Notch model is the best of the standard rate equations; however, for the SPR®660 the standard models are inadequate for a really good fit. The Enhanced Mack model is marginally superior to the others.

In this instance the Enhanced Notch model considerably outperforms the other rate equation in terms of fit; however, this is unsurprising since the model was constructed to address the deficiencies of the existing equations at describing this type of material[16].

Figure 4 compares the SPR®660/MF® CD-26 experimental results with the two best fitting rate equations and Figure 5 does the same for the Ultra-i® 123/MF® CD-26 data.

3.3 248nm Chemically Amplified Photoresists

The UV®26 and UV®113 series photoresists are high activation energy ESCAP materials for KrF exposure tools. UV®26 is a resist designed for implant layers and achieves high aspect ratios at critical dimensions in the order of 300nm and greater, whilst UV®113 is a high resolution logic resist capable of critical dimensions down to 130 nm. Table VII details the parameter values which give optimum fits for each of the four rate equations for the UV®26 data. Table VIII shows the same information for the UV®113 data.

The Enhanced Mack model yields a very poor fit for these materials but the original Mack model gives satisfactory results, as does the Notch rate. In the case of UV®26 the original Mack equation is the best of the conventional models and gives a fair fit. For the UV®113 process, the Notch model is better. Again, the Enhanced Notch rate equation outperforms the other models yielding a good fit to the UV®26 data and an excellent fit to the UV®113.

Figure 6 compares the UV®26/MF® CD-26 experimental results with the two best fitting rate equations whilst Figure 7 does the same for the UV®113/LDD-26W data.

3.4 193nm Chemically Amplified Photoresist

The EPIC V5 photoresist is a state-of-the-art experimental material for ArF exposure for dimensions below 120nm. Table IX details the parameter values which give optimum fits for each of the four rate equations for the V5/MF® CD-26 data. The errors for these fits are somewhat larger than for the other resists, as there is significantly less data available. This is partially due to the fact that ArF materials are typically used at thin film thickness to overcome absorption and aspect ratio issues and is also due to the limitations of the available exposure tool (1.5mm exposure field). Of the three conventional models the Enhanced Mack gives the best fit. Again the Enhanced Notch rate equation yielded a superior fit to the experimental data. Figure 8 compares the V5/MF® CD-26 experimental results with the two best fitting rate equations.

Model							
Original Mack	R_{min}	R_{max}	M_{th}	n			RMSE
	0.048 nm/s	**74.6 nm/s**	**0.487**	**4.415**			**0.0799**
Enhanced Mack	R_{min}	R_{max}	R_{resin}	n	l		RMSE
	0.015 nm/s	**81.6 nm/s**	**5.29 nm/s**	**1.271**	**12.610**		**0.0609**
Original Notch	R_{min}	R_{max}	n	M_{th_notch}	n_notch		RMSE
	0.048 nm/s	**72.7 nm/s**	**-0.196**	**0.467**	**4.563**		**0.0802**
Enhanced Notch	R_{min}	R_{max}	n	M_{th_notch}	n_notch	S	RMSE
	0.016 nm/s	**86.7 nm/s**	**1.441**	**0.663**	**22.591**	**1.38E+8**	**0.0579**

Table III: Optimum rate equation parameters and the RMSE (Root Mean Squared Error) for the SPR®500/MF®-501 Data.

Model							
Original Mack	R_{min} **0.232 nm/s**	R_{max} **183.9 nm/s**	M_{th} **0.684**	n **3.486**			RMSE **0.0868**
Enhanced Mack	R_{min} **0.140 nm/s**	R_{max} **271.2 nm/s**	R_{resin} **32.2 nm/s**	n **1.582**	l **23.577**		RMSE **0.0684**
Original Notch	R_{min} **0.242 nm/s**	R_{max} **202.4 nm/s**	n **0.442**	M_{th_notch} **0.748**	n_notch **3.333**		RMSE **0.0811**
Enhanced Notch	R_{min} **0.152 nm/s**	R_{max} **265.4 nm/s**	n **1.248**	M_{th_notch} **0.824**	n_notch **8.588**	S **1.74E+10**	RMSE **0.0621**

Table IV: Optimum rate equation parameters and the RMSE (Root Mean Squared Error) for the SPR®850/MF® CD-26 Data.

Model							
Original Mack	R_{min} **0.084 nm/s**	R_{max} **144.2 nm/s**	M_{th} **0.291**	n **6.530**			RMSE **0.1120**
Enhanced Mack	R_{min} **0.038 nm/s**	R_{max} **176.2 nm/s**	R_{resin} **6.09 nm/s**	n **3.327**	l **6.625**		RMSE **0.1039**
Original Notch	R_{min} **0.089 nm/s**	R_{max} **152.6 nm/s**	n **1.297**	M_{th_notch} **0.393**	n_notch **5.745**		RMSE **0.1107**
Enhanced Notch	R_{min} **0.046 nm/s**	R_{max} **161.4 nm/s**	n **2.740**	M_{th_notch} **0.574**	n_notch **17.29**	S **845**	RMSE **0.0698**

Table V: Optimum rate equation parameters and the RMSE (Root Mean Squared Error) for the SPR®660/MF® CD-26 Data.

Model							
Original Mack	R_{min} **0.060 nm/s**	R_{max} **67.5 nm/s**	M_{th} **0.560**	n **11.528**			RMSE **0.1257**
Enhanced Mack	R_{min} **0.017 nm/s**	R_{max} **133.1 nm/s**	R_{resin} **13.90 nm/s**	n **2.552**	l **10.579**		RMSE **0.2000**
Original Notch	R_{min} **0.062 nm/s**	R_{max} **109.0 nm/s**	n **1.771**	M_{th_notch} **0.634**	n_notch **13.44**		RMSE **0.0927**
Enhanced Notch	R_{min} **0.036 nm/s**	R_{max} **115.6 nm/s**	n **1.970**	M_{th_notch} **0.650**	n_notch **20.67**	S **201**	RMSE **0.0542**

Table VI: Optimum rate equation parameters and the RMSE (Root Mean Squared Error) for the Ultra-i® 123/MF® CD-26 Data.

Model							
Original Mack	R_{min} **0.038 nm/s**	R_{max} **2999 nm/s**	M_{th} **0.280**	n **10.825**			RMSE **0.1357**
Enhanced Mack	R_{min} **0.018 nm/s**	R_{max} **3004 nm/s**	R_{resin} **62.32 nm/s**	n **3.665**	l **8.991**		RMSE **0.2146**
Original Notch	R_{min} **0.039 nm/s**	R_{max} **10015 nm/s**	n **4.815**	M_{th_notch} **0.371**	n_notch **6.657**		RMSE **0.1360**
Enhanced Notch	R_{min} **0.029 nm/s**	R_{max} **10014 nm/s**	n **6.07**	M_{th_notch} **0.489**	n_notch **8.478**	S **189**	RMSE **0.0991**

Table VII: Optimum rate equation parameters and the RMSE (Root Mean Squared Error) for the UV®26/MF® CD-26 Data.

Model							RMSE
Original Mack	R_{min}	R_{max}	M_{th}	n			RMSE
	0.0180 nm/s	**640.0 nm/s**	**0.280**	**10.825**			**0.1357**
Enhanced Mack	R_{min}	R_{max}	R_{resin}	n	l		RMSE
	0.0005 nm/s	**907.9 nm/s**	**358.2 nm/s**	**2.745**	**13.535**		**0.2903**
Original Notch	R_{min}	R_{max}	n	M_{th_notch}	n_notch		RMSE
	0.0180 nm/s	**841.7 nm/s**	**1.338**	**0.482**	**69.528**		**0.0758**
Enhanced Notch	R_{min}	R_{max}	n	M_{th_notch}	n_notch	S	RMSE
	0.0090 nm/s	**841.7 nm/s**	**1.339**	**0.482**	**70.414**	**15.1**	**0.0673**

Table VIII: Optimum rate equation parameters and the RMSE (Root Mean Squared Error) for the UV®113 V5/MF® CD-26 Data.

Model							RMSE
Original Mack	R_{min}	R_{max}	M_{th}	n			RMSE
	0.0012 nm/s	**5764 nm/s**	**0.259**	**19.930**			**0.5296**
Enhanced Mack	R_{min}	R_{max}	R_{resin}	n	l		RMSE
	0.0004 nm/s	**6000 nm/s**	**99.0 nm/s**	**5.476**	**11.027**		**0.4840**
Original Notch	R_{min}	R_{max}	n	M_{th_notch}	n_notch		RMSE
	0.0012 nm/s	**6000 nm/s**	**1.486**	**0.276**	**18.469**		**0.53322**
Enhanced Notch	R_{min}	R_{max}	n	M_{th_notch}	n_notch	S	RMSE
	0.0005 nm/s	**13149 nm/s**	**6.176**	**0.412**	**33.358**	**1.18E+4**	**0.4102**

Table IX: Optimum rate equation parameters and the RMSE (Root Mean Squared Error) for the EPIC V5/MF® CD-26 Data.

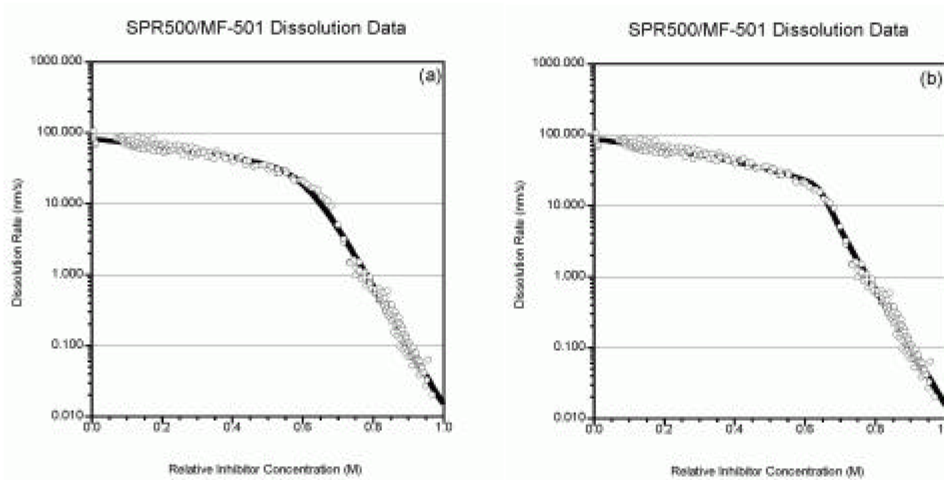

Figure 2: The SPR®500/MF®-501 experimental data plotted with (a) the optimum fit of the Enhanced Mack rate equation and (b) the optimum fit of the Enhanced Notch equation.

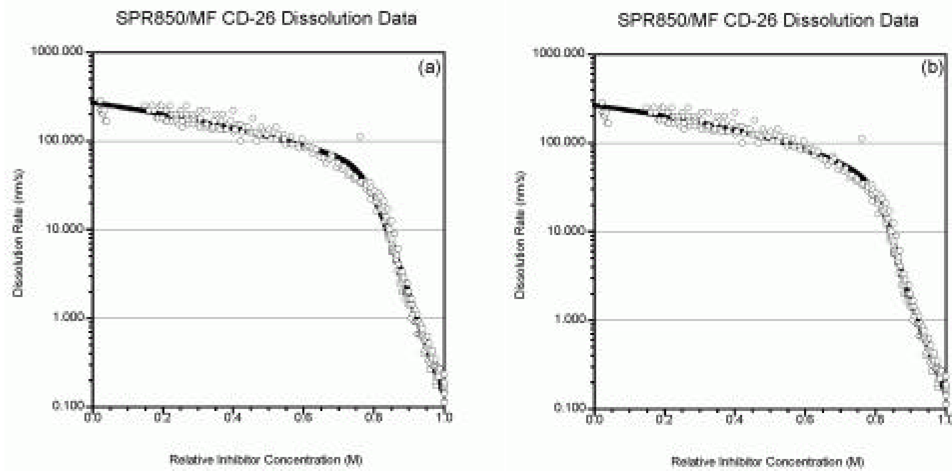

Figure 3: The SPR®850/MF® CD-26 experimental data plotted with (a) the optimum fit of the Enhanced Mack rate equation and (b) the optimum fit of the Enhanced Notch equation.

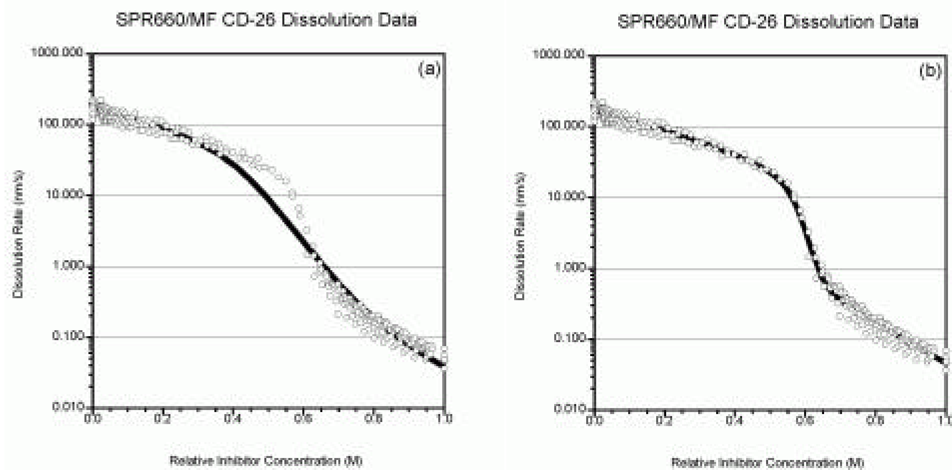

Figure 4: The SPR®660/MF® CD-26 experimental data plotted with (a) the optimum fit of the Enhanced Mack rate equation and (b) the optimum fit of the Enhanced Notch equation.

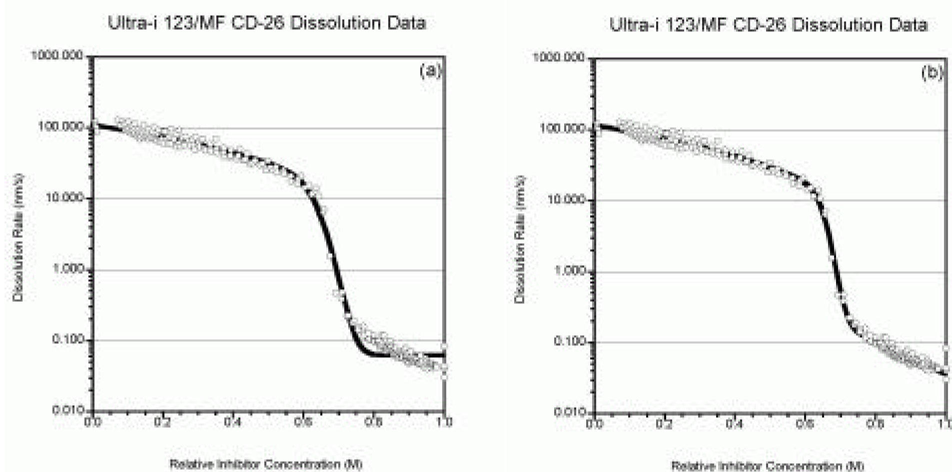

Figure 5: The Ultra-i® 123/MF® CD-26 experimental data plotted with (a) the optimum fit of the Notch rate equation

and (b) the optimum fit of the Enhanced Notch equation.

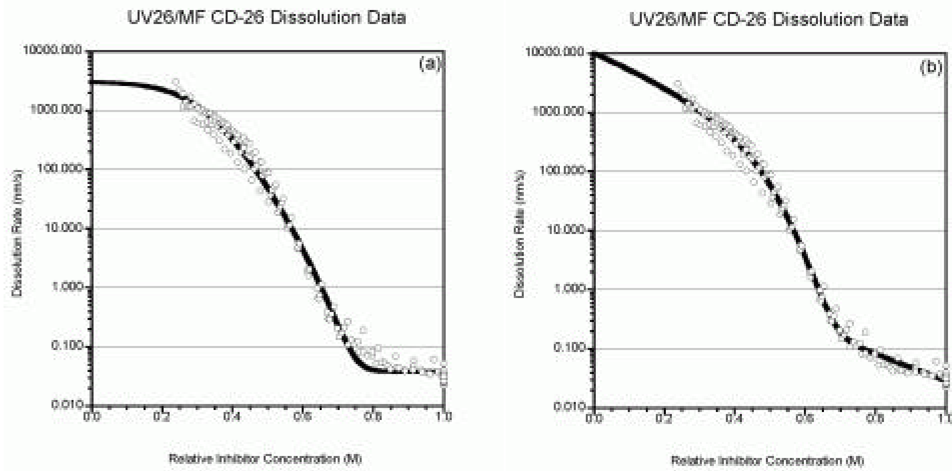

Figure 6: The UV®26/MF® CD-26 experimental data plotted with (a) the optimum fit of the Mack rate equation and (b) the optimum fit of the Enhanced Notch equation.

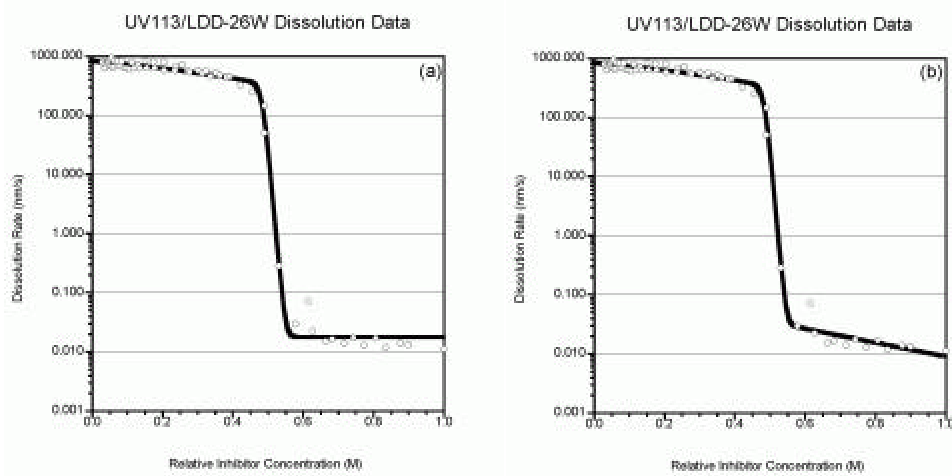

Figure 7: The UV®113/LDD-26W experimental data plotted with (a) the optimum fit of the Notch rate equation and (b) the optimum fit of the Enhanced Notch equation.

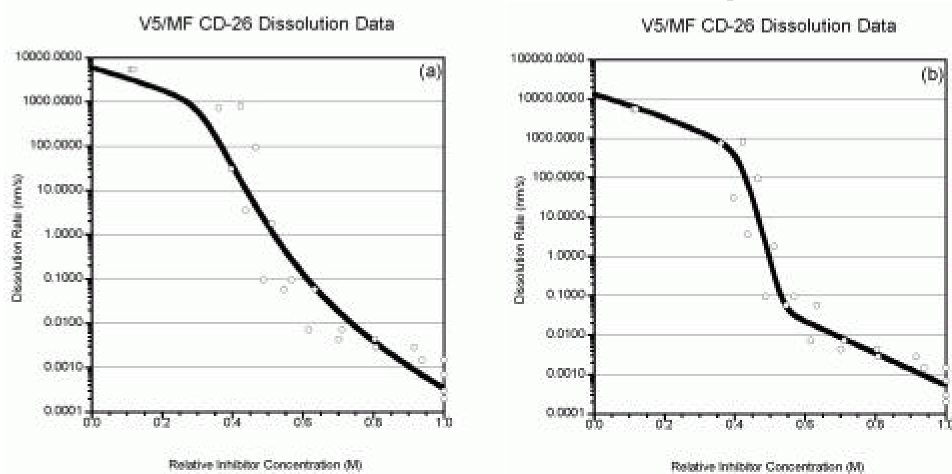

Figure 8: The EPIC V5/MF® CD-26 experimental data plotted with (a) the optimum fit of the Enhanced Mack rate equation and (b) the optimum fit of the Enhanced Notch equation.

5. DISCUSSION ON RATE EQUATION FITTING

Before going on to discuss the utility of the rate equations that have been studied, it is worth considering a few key points. Previous work[17] noted that for a rate equation to predict the general performance of a particular process it need only accurately represent a small, but critical, part of the materials dissolution response. This critical region is typically the part of the dissolution response exhibiting the highest discrimination, e.g. the notch region in a high resolution novolak material. A further study[16] showed that even relatively subtle changes in the shape of the dissolution rate curve at low development rates can have small yet significant impact on the predicted process window.

During this work the rate equations have been fitted to experimental data by error minimization; however, inspection of Figures 2 through 8 reveals that in many cases the majority of data points are in the regions near R_{min} and R_{max}, whilst very few are in the "critical" region where discrimination is highest. Thus the fits produced may be numerically optimum but they might not be optimum in terms of reproducing the behavior of the lithographic process, i.e. the "best" fit may not be a "good" fit.

Overcoming this problem requires either a sophisticated weighting strategy or a completely manual fitting process. Since the weighting system would need to be varied on a case-by-case basis and manual fitting is inherently subjective neither option facilitates easy automation of the fitting process.

As an example, when Figure 4(a) is inspected, it is clearly visible that the large number of points at low and high dissolution rates are dominating the fit of the Enhanced Mack equation. Since the transition region from high to low rates is badly represented in this example it is unlikely that this model would simulate results representative of the actual process. The resist could probably be simulated reasonably well using either the original Mack model or the standard Notch model; however, the parameters required to do so would be different from those decided by the least squares fit to the whole datset.

6. CONCLUSIONS

Four rate equations have been fitted to experimental dissolution rate versus M data for a wide variety of photoresist types. Whilst one of the commonly used rate equations gave a reasonable fit most cases (with the exception of the SPR660 process), it was the Enhanced Notch model which gave the best fit for every example studied. Inspection of Figures 2(b) through 8(b) reveals that not only were the fits numerically the best, but also that each appears to be a "good" fit, replicating all the behaviors exhibited in the experimental data.

Whilst it is possible that the Enhanced Notch rate equation cannot describe all resist processes (low activation chemically amplified photoresist has not been tested), it would appear that it is flexible enough to model most materials. Additionally, since it appears to be able to conform to the shape of the experimental data, straight forward numerical fitting techniques without specialized weighting functions can be implemented, as it always catches the nuances of the critical region.

Whilst researchers from NEC[13] have proposed a model flexible enough to fit nearly any data set, the Enhanced Notch equation has the advantage of using only 6 parameters (versus 9) and that each of the values has either a physical or an implied meaning.

ACKNOWLEDGEMENTS

The authors would like to thank Doris Kang of Shipley Company and Catherine Swible-Keane formerly of Shipley Company for their assistance in generating the experimental results.

REFERENCES

1. F.H. Dill. "Optical Lithography", *IEEE Transactions on Electron Devices*, ED-22(7), pp. 440 – 444, 1975.
2. F.H. Dill, Hornberger, P.S. Hauge and J.M. Shaw. "Characterization of positive photoresist", *IEEE Transactions on Electron Devices*, ED-22(7), pp. 445 – 452, 1975.
3. K.L. Konnerth and F.H. Dill. "In-situ measurement of dielectric thickness during etching or developing processes", *IEEE Transactions on Electron Devices*, ED-22(7), pp. 452 – 456, 1975.
4. F.H. Dill, A.R. Neureuther, J.A. Tuttle and E.J. Walker. "Modeling projection printing of positive photoresists", *IEEE Transactions on Electron Devices*, ED-22(7), pp. 456 – 464, 1975.

5. C.A. Mack, “Advanced topics in lithography modeling”, *Advances in Resist Technology and Processing III*, pp. 276 – 285, SPIE Vol. 631, 1986.

6. D.J. Kim, W.G. Oldham and A.R. Neureuther, “Development of positive photoresist”, *IEEE Transactions on Electron Devices*, ED-31(12), pp. 1730 – 1735, 1984.

7. S.A. Robertson, J.T.M. Stevenson, R.J. Holwill, S.G. Hansen, C.E. Ebersole, M. Thirsk and I.S. Daraktchiev. “The modelling of post exposure bake and surface inhibition effects in positive photoresist using absolute thickness data”, *Advances in Resist Technology and Processing IX*, pp.540 – 552. SPIE Vol. 1672, 1992.

8. C.A Mack. “Development of positive photoresists”, *Journal of the Electrochemical Society; Solid-state Science and Technology*, Vol.134, No. 1, pp. 148 - 152, 1987.

9. G.Arthur, C.Wallace and B.Martin, “A comparison of Recent Development Models in Optical Lithography Simulation”, *SPIE Vol. 3332*, pp. 538-549, 1998.

10. G.Arthur, C.A.Mack and B.Martin, “A New Development Model for Lithography Simulation”, *Olin Microlithography Seminar, Interface ’97*, pp. 55-66, November, 1997.

11. C.A.Mack and G.Arthur, “Notch Model for Photoresist Dissolution”, *Electrochemical and Solid-State Letters*,1 (2), pp. 86-88 (1998)

12. S.G. Hansen, G. Dao, H. Gaw, Q. Qian, P. Spragg and R.J. Hurditch. “Study of the relationship between exposure margin and photolithographic process latitude and mask linearity”, *Optical/Laser Microlithography IV*, pp. 230 – 244, SPIE Vol. 1463, 1991.

13. T. Ohfuji, K. Yamanaka and M. Sakamoto. “Characterization and modeling of high resolution positive photoresists” *Advances in Resist Technology and Processing V*, pp. 190 – 197, SPIE Vol. 920, 1988.

14. C.A. Mack. “New Kinetic Model for Resist Dissolution”, *Journal of the Electrochemical Society*, Vol. 139, No. 4, pp. L35, 1992

15. M.A. Toukhy, S.G. Hansen, R.J. Hurditch and C.A. Mack. “Experimental Investigation of a novel dissolution model”, *Advances in Resist Technology and Processing IX*, pp. 286 - 298, SPIE Vol. 1672, 1992.

16. S.A. Robertson, E.K. Pavelchek, W. Hoppe and R. Wildfeuer, “An improved Notch model for resist dissolution in lithography simulation”, Advances in Resist Technology and Processing XVII, Paper 4345-108, SPIE Vol. 4345, 2001.

17. S.A. Robertson, E.K. Pavelchek, C.I. Swible-Keane, J.R. Bohland and M.T. Reilly. “Factors affecting pitch bias in lithography simulation”, *Optical Microlithography XIII*, pp. 744 – 758, SPIE Vol. 4000, 2000.